CHAPTER 3

Results

Experiment I

3.1 Field Collections and Establishment of Isoline Colonies

Samples of fully engorged females of *An. paraliae* were collected from cow-baited traps in 4 provinces of Thailand (Figure 3.1, Table 3.1). A total of 16 isolines were established and maintained in an insectary at Chiang Mai University, and they were used for studies on metaphase karyotype, cross-mating experiments and molecular analysis.

3.2 Metaphase Karyotype of *Anopheles paraliae*

Cytogenetic observation of F_1- and/or F_2- progenies of the 16 isolines which were represented in 4 provinces across 3 regions (western, eastern, southern) in Thailand, demonstrated that *An. paraliae* has the typical chromosome number of 2n = 6, consisting of two pairs of autosomes (submetacentric and metacentric) and one pair of heteromorphic sex chromosomes (XX in females and XY in males). Based on the number and amount of major block(s) of the heterochromatin present in the heterochromatic arm of the sex chromosomes, 3 types of X (X_1, X_2, X_3) and 5 types of Y (Y_1, Y_2, Y_3, Y_4, Y_5) chromosomes were obtained in this investigation (Figure 3.2-3.3 and Table 3.1). The X_1 chromosome has a small metacentric shape with one arm euchromatic, and the opposite one totally heterochromatic. The X_2 chromosome is different from the X_1 chromosome in having an extra block of heterochromatin in the heterochromatic arm, making it a long arm of submetacentric configuration. The X_3 chromosome has a large submetracentric shape that was slightly different from the X_2 chromosome in having an extra block of heterochromatin at the distal end of the long heterochromatic arm. A good comparison of the size and shape between X_2 and X_3

chromosomes can be seen in heterozygous females (Figure 3.2j). Similar to the situation in the X chromosome, the Y chromosome also exhibited extensive variation in size and shape, due to differing amounts and distribution of heterochromatic block. Thus, the Y_1 chromosome is a small telocentric figure, which probably represents the simple or ancestral form of the Y chromosome (Figure 3.2a). The Y_2 chromosome has a small subtelocentric or acrocentric shape that slightly differs from the Y_1 chromosome which has a very small portion of the short arm present (Figure 3.2b-d). Chromosome Y_3 has a large subtelocentric shape that obviously differs from the Y_2 chromosome in having an extra block of heterochromatin at the distal end of the long heterochromatic arm (Figure 3.2f). The Y_4 chromosome is clearly submetacentric, with the short arm approximately 1/3 the length of the long arm. It appears to have derived from the Y_3 chromosome by means of adding an extra block of heterochromatin onto the short arm, and transferring it to a submetacentric configuration (Figure 3.2g-i). Chromosome Y_5 has a medium metacentric configuration, which is slightly shorter than that in the Y_4 chromosome. It could have arisen from the ancestral Y_1 chromosome simply through additional of 2 extra blocks of heterochromatin onto the opposite long arm (Figure 3.2k). Hence, 5 karyotypic forms were recognized based on unique characteristics of the X and Y chromosomes and they were designated as Forms A (X_3, Y_1), B (X_1, X_2, X_3, Y_2), C (X_3, Y_3), D (X_1, X_2, X_3, Y_4) and E (X_3, Y_5).

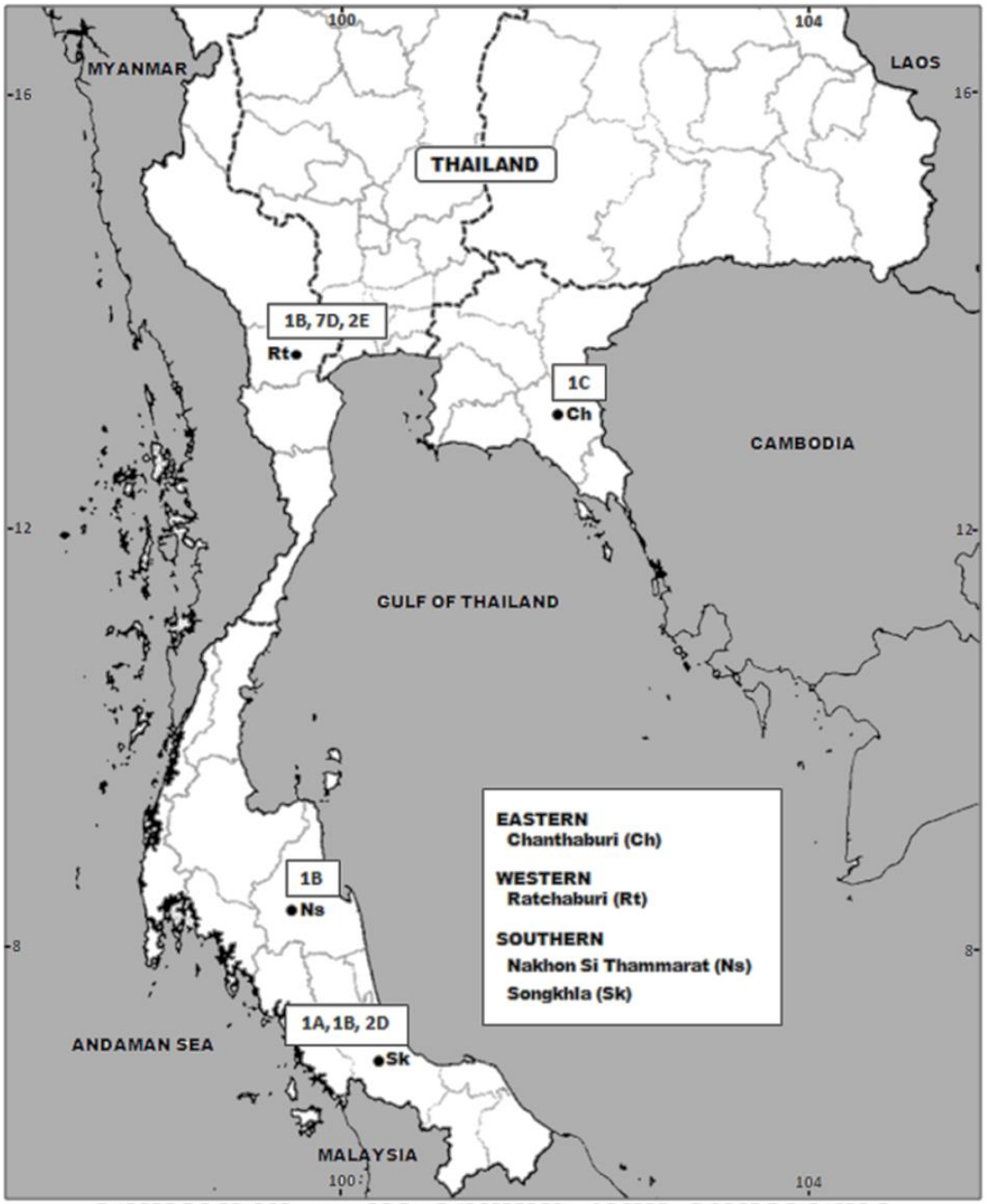

Figure 3.1 Map of Thailand showing 4 provinces where samples of *An. paraliae* were collected and the numbers of isolines of the 5 karyotypic forms (A-E) were detected

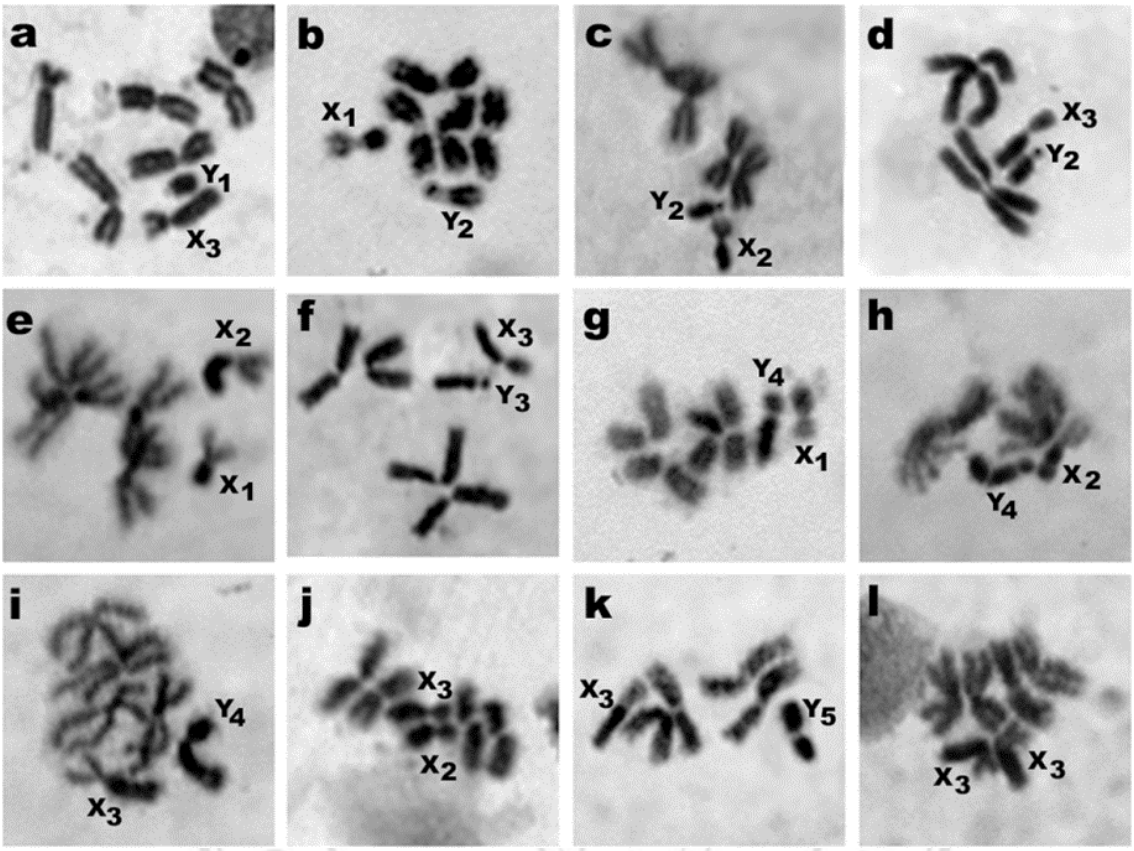

Figure 3.2 Metaphase karyotypic forms of *An. paraliae*. (a) Form A (X_3, Y_1), (b) Form B (X_1, Y_2), (c) Form B (X_2, Y_2), (d) Form B (X_3, Y_2), (e) Form B (X_1, X_2), (f) Form C (X_3, Y_3), (g) Form D (X_1, Y_4), (h) Form D (X_2, Y_4), (i) Form D (X_3, Y_4), (j) Form D (X_2, X_3), (k) Form E (X_3, Y_5), (l) Form E (X_3, X_3)

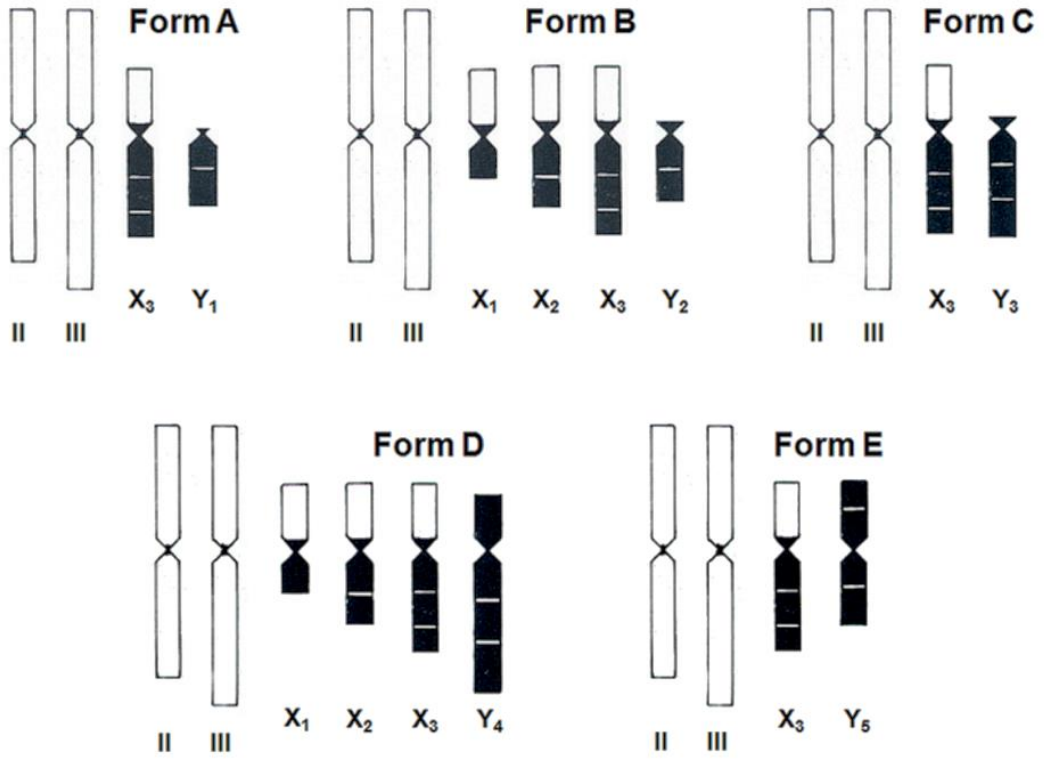

Figure 3.3 Diagrams of representative metaphase karyotypes of Forms A, B, C, D and E of *An. paraliae*

Table 3.1 Locations in 4 provinces of Thailand, code of isolines, 5 karyotypic forms (A-E) of *An. paraliae* and their GenBank accession numbers

Location (Geographical coordinate)	Code of isoline[a]	Karyotypic form	DNA Region	GenBank accession number			Reference
				ITS2	COI	COII	
An. paraliae							
Chanthaburi (12° 38′ N, 102° 12′ E)	Ch1C[a]	C (X_3, Y_3)	ITS2, COI, COII	AB733475	AB733491	AB733507	This study
Ratchaburi (13° 30′ N, 99° 54′ E)	Rt1D	D (X_3, Y_4)	ITS2, COI, COII	AB733476	AB733492	AB733508	This study
	Rt2D	D (X_3, Y_4)	ITS2, COI, COII	AB733477	AB733493	AB733509	This study
	Rt3D	D (X_3, Y_4)	ITS2, COI, COII	AB733478	AB733494	AB733510	This study
	Rt4B[a]	B (X_2, Y_2)	ITS2, COI, COII	AB733479	AB733495	AB733511	This study
	Rt5E[a]	E (X_3, Y_5)	ITS2, COI, COII	AB733480	AB733496	AB733512	This study
	Rt6D	D (X_3, Y_4)	ITS2, COI, COII	AB733481	AB733497	AB733513	This study
	Rt7D[a]	D (X_2, Y_4)	ITS2, COI, COII	AB733482	AB733498	AB733514	This study
	Rt8D[a]	D (X_1, Y_4)	ITS2, COI, COII	AB733483	AB733499	AB733515	This study
	Rt9E	E (X_3, Y_5)	ITS2, COI, COII	AB733484	AB733500	AB733516	This study
	Rt10D	D (X_3, Y_4)	ITS2, COI, COII	AB733485	AB733501	AB733517	This study

Table 3.1 (continued)

Location (Geographical coordinate)	Code of isoline[a]	Karyotypic form	DNA Region	GenBank accession number			Reference
				ITS2	COI	COII	
Nakhon Si Thammarat (08° 29′ N, 100° 0′ E)	Ns1B[a]	B (X_3, Y_2)	ITS2, COI, COII	AB733486	AB733502	AB733518	This study
Songkhla (07° 13′ N, 100° 37′ E)	Sk1B	B (X_1, Y_2)	ITS2, COI, COII	AB733487	AB733503	AB733519	This study
	Sk2D	D (X_1, Y_4)	ITS2, COI, COII	AB733488	AB733504	AB733520	This study
	Sk3A[a]	A (X_3, Y_1)	ITS2, COI, COII	AB733489	AB733505	AB733521	This study
	Sk4D	D (X_3, Y_4)	ITS2, COI, COII	AB733490	AB733506	AB733522	This study
An. sinensis	i2ACM	A (X, Y_1)	ITS2	AY130473	-	-	Min et al. 2002
	-	B (X, Y_2)	COI	-	AY444351	-	Park et al. 2003
	i1BKR	B (X, Y_2)	COII	-	-	AY130464	Min et al. 2002
An. pullus	-	A (X_1, X_2, Y_2)	ITS2, COI, COII	AY444345	AY444348	AY444347	Park et al. 2003
An. peditaeniatus	RbB	B (X_3, Y_2)	ITS2, COI, COII	AB539061	AB539069	AB539077	Choochote 2011

[a] used in cross-mating experiments

3.3 Cross-mating Experiments

Details of hatchability, pupation, emergence and adult sex ratio of parental, reciprocal and F_1-hybrid experiments among the 7 isolines of *An. paraliae* representing Forms A-E are shown in Table 3.2. All crosses gave viable progenies through the F_2-generations. No evidence of genetic incompatibility and/or post-mating reproductive isolation was observed among these crosses. The salivary gland polytene chromosomes of the hybrid larvae from all crosses showed complete synapsis without inversion loops in all chromosome arms (Figure 3.4).

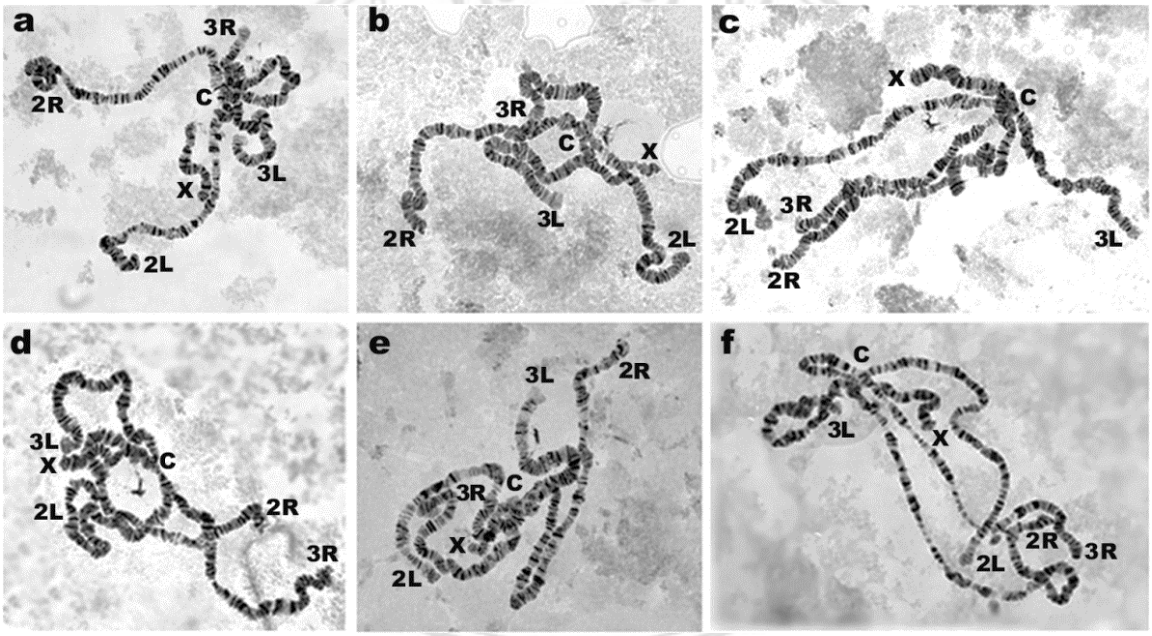

Figure 3.4 Complete synapsis in all arms of salivary gland polytene chromosomes of F_1-hybrids of *An. paraliae*. (a) Sk3A female x Ns1B male; (b) Sk3A female x Rt4B male; (c) Sk3A female x Ch1C male; (d) Sk3A female x Rt7D male; (e) Sk3A female x Rt8D male; (f) Sk3A female x Rt5E male

Table 3.2 Cross-mating experiments among 7 isolines of *An. paraliae*

Crosses (Female x Male)	Total eggs (number)[a]	Embryonation rate[b]	Hatched n (%)	Pupation n (%)	Emergence n (%)	Total emergence n (%)	
						Female	Male
Parental cross							
Sk3A x Sk3A	316 (158, 158)	84	231 (73.10)	212 (91.77)	208 (98.11)	120 (57.69)	88 (42.31)
Ns1B x Ns1B	319 (162, 157)	83	258 (80.88)	248 (96.12)	199 (80.24)	121 (60.80)	78 (39.20)
Rt4B x Rt4B	372 (150, 222)	84	305 (81.99)	305 (100.00)	305 (100.00)	143 (46.89)	162 (53.11)
Ch1C x Ch1C	394 (187, 207)	82	315 (79.95)	277 (87.94)	265 (95.67)	151 (56.98)	114 (43.02)
Rt7D x Rt7D	285 (167, 118)	92	242 (84.91)	242 (100.00)	220 (90.91)	116 (52.73)	104 (47.27)
Rt8D x Rt8D	299 (190, 109)	85	245 (81.94)	213 (86.94)	196 (92.02)	83 (42.35)	113 (57.65)
Rt5E x Rt5E	309 (147, 162)	81	226 (73.14)	212 (93.80)	208 (98.11)	106 (50.96)	102 (49.04)
Reciprocal cross							
Sk3A x Ns1B	346 (186, 160)	73	242 (69.94)	213 (88.02)	194 (91.08)	97 (50.00)	97 (50.00)
Ns1B x Sk3A	359 (158, 201)	75	266 (74.09)	231 (86.84)	204 (88.31)	106 (51.96)	98 (48.04)
Sk3A x Rt4B	339 (157, 182)	89	295 (87.02)	289 (97.97)	274 (94.81)	162 (59.12)	112 (40.88)
Rt4B x Sk3A	391 (194, 197)	90	344 (87.98)	310 (90.12)	292 (94.19)	110 (37.67)	182 (62.33)

Table 3.2 (continued)

Crosses (Female x Male)	Total eggs (number)[a]	Embryonation rate[b]	Hatched n (%)	Pupation n (%)	Emergence n (%)	Total emergence n (%)	
						Female	Male
Sk3A x Ch1C	344 (189, 155)	90	299 (86.92)	299 (100.00)	275 (91.97)	121 (44.00)	154 (56.00)
Ch1C x Sk3A	331 (206, 125)	96	314 (94.86)	314 (100.00)	308 (98.09)	135 (43.83)	173 (56.17)
Sk3A x Rt7D	348 (158, 190)	88	306 (87.93)	278 (90.85)	272 (97.84)	131 (48.16)	141 (51.84)
Rt7D x Sk3A	325 (125, 200)	90	260 (80.00)	260 100.00)	260 (100.00)	130 (50.00)	130 (50.00)
Sk3A x Rt8D	347 (157, 190)	84	232 (66.86)	204 (87.93)	200 (98.04)	93 (46.50)	107 (53.50)
Rt8D x Sk3A	305 (147, 158)	82	247 (80.98)	247 (100.00)	237 (95.95)	117 (49.37)	120 (50.63)
Sk3A x Rt5E	353 (167, 186)	86	297 (84.13)	273 (91.92)	273 (100.00)	134 (49.08)	139 (50.92)
Rt5E x Sk3A	376 (194, 182)	82	293 (77.92)	293 (100.00)	293 (100.00)	126 (43.00)	167 (57.00)
F_1- hybrid cross							
(Sk3A x Ns1B)F_1 x (Sk3A x Ns1B)F_1	309 (109, 200)	78	229 (74.11)	199 (86.90)	192 (96.48)	89 (46.35)	103 (53.65)
(Ns1B x Sk3A)F_1 x (Ns1B x Sk3A)F_1	308 (194, 114)	98	274 (88.96)	186 (67.88)	186 (100.00)	129 (69.35)	57 (30.65)
(Sk3A x Rt4B)F_1 x (Sk3A x Rt4B)F_1	350 (155, 195)	93	301 (86.00)	256 (85.05)	250 (97.66)	117 (46.80)	133 (53.20)

Table 3.2 (continued)

Crosses (Female x Male)	Total eggs (number)[a]	Embryonation rate[b]	Hatched n (%)	Pupation n (%)	Emergence n (%)	Total emergence n (%)	
						Female	Male
(Rt4B x Sk3A)F_1 x (Rt4B x Sk3A)F_1	383 (220, 163)	94	326 (85.12)	297 (91.10)	293 (98.65)	140 (47.78)	153 (52.22)
(Sk3A x Ch1C)F_1 x (Sk3A x Ch1C)F_1	345 (150, 195)	76	228	228 (100.00)	221 (96.93)	93 (42.08)	128 (57.92)
(Ch1C x Sk3A)F_1 x (Ch1C x Sk3A)F_1	248 (118, 130)	80	169 (68.14)	169 (100.00)	169 (100.00)	73 (43.20)	96 (56.80)
(Sk3A x Rt7D)F_1 x (Sk3A x Rt7D)F_1	406 (220, 186)	73	252 (62.07)	244 (96.83)	224 (91.80)	98 (43.75)	126 (56.25)
(Rt7D x Sk3A)F_1 x (Rt7D x Sk3A)F_1	351 (189, 162)	76	253 (72.08)	253 (100.00)	248 (98.02)	137 (55.24)	111 (44.76)
(Sk3A x Rt8D)F_1 x (Sk3A x Rt8D)F_1	391 (209, 182)	67	242 (61.89)	242 (100.00)	240 (99.17)	120 (50.00)	120 (50.00)
(Rt8D x Sk3A)F_1 x (Rt8D x Sk3A)F_1	334 (148, 186)	72	230 (68.86)	223 (96.96)	216 (96.86)	115 (53.24)	101 (46.76)
(Sk3A x Rt5E)F_1 x (Sk3A x Rt5E)F_1	403 (209, 194)	92	363 (90.07)	341 (93.94)	319 (93.55)	145 (45.45)	174 (54.55)
(Rt5E x Sk3A)F_1 x (Rt5E x Sk3A)F_1	405 (220, 185)	87	344 (84.94)	289 (84.01)	282 (97.58)	189 (67.02)	93 (32.98)

a: Two selective egg-batches of inseminated females from each cross; *b*: dissection from 100 eggs; n = number

3.4 DNA Sequence and Phylogenetic Analysis

DNA sequences of the ITS2, COI and COII of the 16 isolines of *An. paraliae* Forms A-E were analysed. They all showed the same lengths for ITS2 (448 bp), COI (658 bp) and COII (685 bp) sequences. All 5 karyotypic forms showed completely identical of ITS2 sequences. Neighbor-joining (NJ) trees were constructed in order to determine genetic relationships among the 5 karyotypic forms (Figure 3.5). The 16 isolines were monophyletic with high supported in NJ tree (bootstrap values 100%). Obviously, the mean genetic distance within and between the 5 karyotypic forms exhibited no significant difference (0.000-0.002) in these DNA regions. However, the trees for ITS2, COI and COII of these isolines (Forms A-E) were clearly different from the 3 species members of the Hyrcanus Group, i.e., *An. peditaeniatus*, *An. pullus* and *An. sinensis*, with strongly supported bootstrap values (100%).

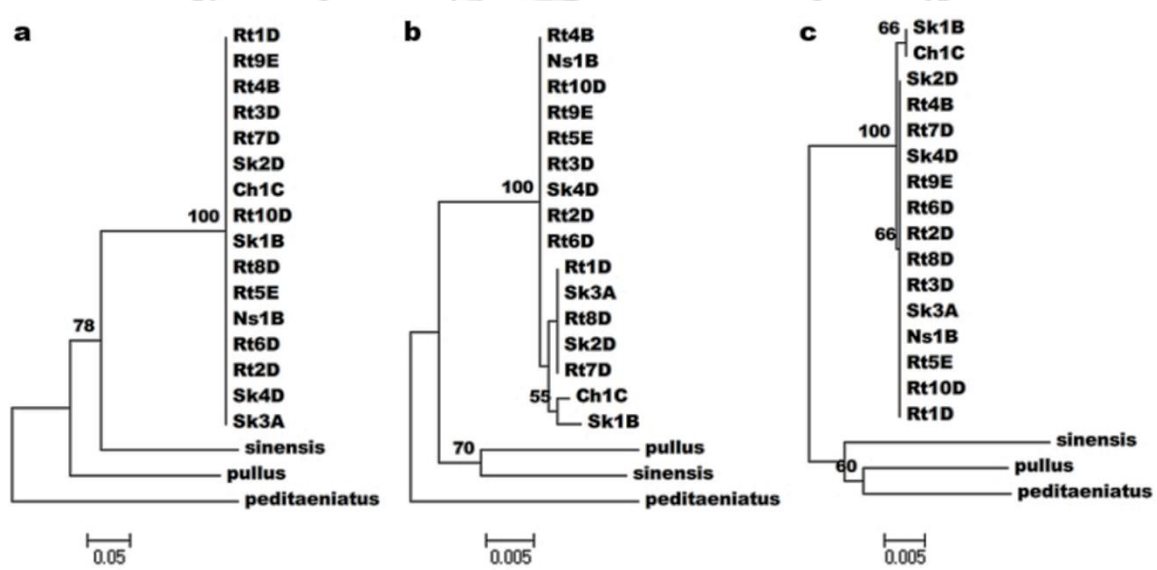

Figure 3.5 Neighbor-joining (NJ) trees inferred from sequences of 3 loci (a) ITS2, (b) COI and (c) COII of the 16 isolines of *An. paraliae* compared with *An. peditaeniatus*, *An. pullus* and *An. sinensis*. Numbers on branches are bootstrap values (%) after 1,000 replications. Bootstrap values under 50% not shown. Branch lengths are proportional to genetic distance (scale bar)

Experiment II

3.5 Morphological Identification

The morphological characteristics of adult female that distinguished *An. lesteri* from *An. paraliae* were shown in Figure 3.6. The wing of *An. lesteri* from Korea showing wide pale fringe spot extending from tip of vein R_1 to R_{4+5}, and 2 dark spots on anal vein (1A), whereas, wings of *An. paraliae* from Thailand showing very narrow pale fringe spot at tip of vein R_2, and 2 dark spots on 1A similar to that of *An. lesteri*, narrow fringe spot at tip of vein R_2, and 2 dark spots on 1A, and moderated fringe spot extending from tip of vein R_{1-3}, and 1 dark spot on 1A.

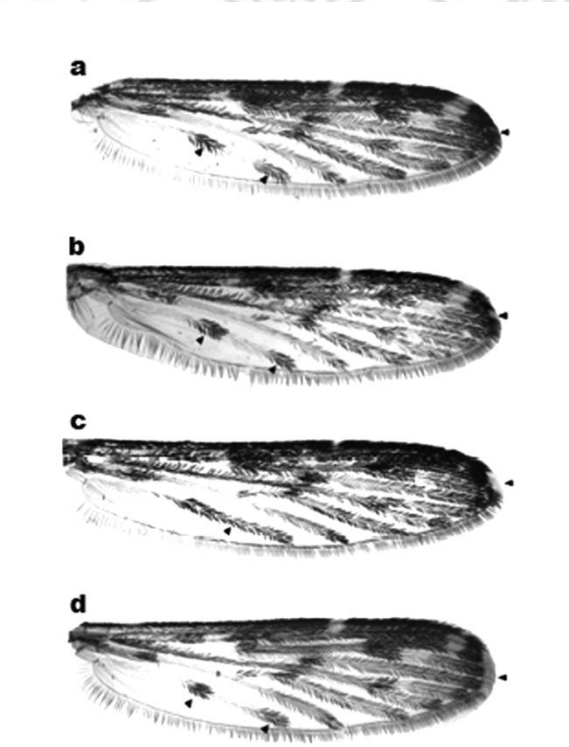

Figure 3.6 (a-c) Wings of *An. paraliae* from Thailand showing: (a) very narrow pale fringe spot at tip of vein R_2, and 2 dark spots on 1A similar to that of *An. lesteri*, (b) narrow fringe spot at tip of vein R_2, and 2 dark spots on 1A, (c) moderated fringe spot extending from tip of vein R_{1-3}, and 1 dark spot on 1A, and (d) Wing of *An. lesteri* from Korea showing wide pale fringe spot extending from tip of vein R_1 to R_{4+5}, and 2 dark spots on anal vein (1A)

3.6 Establishment of Isoline Colonies

Three and 5 isolines of *An. lesteri* (ilG1, ilG2, ilG3) and *An. paraliae* (ipR1, ipR2, ipN1, ipS1, ipS2), respectively, were established successfully, and maintained in colonies for more than 5 consecutive generations in our laboratory. They were used for crossing experiments and comparative DNA sequence analyses.

3.7 Cross-mating Experiments

Details of hatchability, pupation, emergence and adult sex-ratio of parental, reciprocal and F_1-hybrid crosses between *An. lesteri* from Korea and *An. paraliae* from Thailand are shown in Table 3.3. All crosses yielded viable progenies through the F_2-generations. No evidence of genetic incompatibility and/or post-mating reproductive isolation was observed among these crosses (repeated twice: experiments 2 and 3, data are not shown). The salivary gland polytene chromosomes of F_1-hybrid larvae from all crosses showed complete synapsis without inversion loops in all chromosome arms (Figure 3.7).

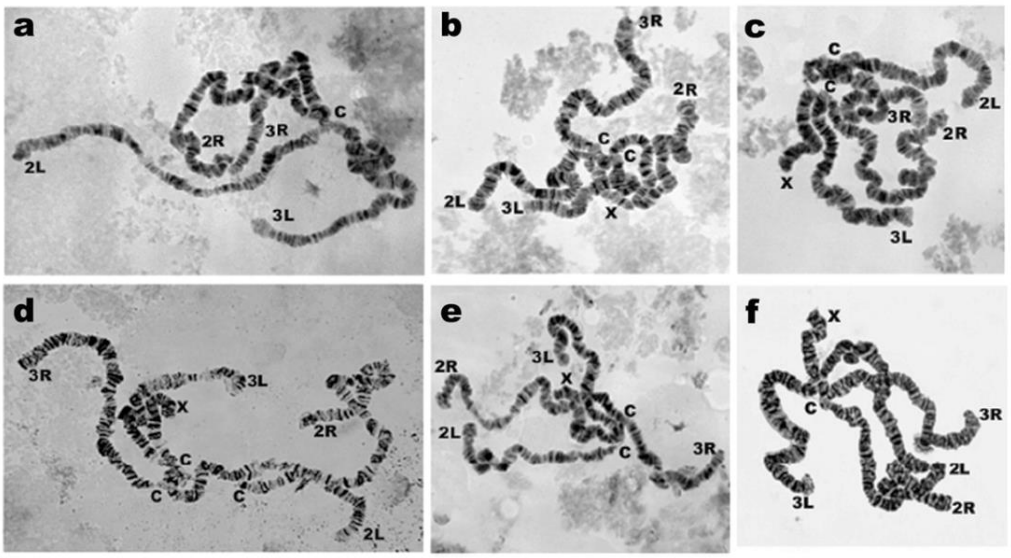

Figure 3.7 Complete synapsis in all arms of salivary gland polytene chromosome of F_1-hybrid larvae of crosses between *An. lesteri* and *An. paraliae*. A: ilG1 female x ipN1 male; B: ilG1 female x ipR1 male; C: ipR1 female x ilG1 male; D: ipS1 female x ilG1 male; E: ipN1 female x ilG1 male; F: ilG1 female x ipS1 male

Table 3.3 Cross-mating experiments among the 4 isolines of *An. lesteri* and *An. paraliae*

Crosses (Female x Male)	Total eggs (number)[a]	Embryonation rate[b]	Hatched n (%)	Pupation n (%)	Emergence n (%)	Total emergence n (%)	
						Female	Male
Parental cross							
ilG1 x ilG1	345 (155, 190)	65	221 (64.05)	221 (100.00)	221 (100.00)	111 (50.23)	110 (49.77)
ipR1 x ipR1	352 (194, 158)	84	296 (84.09)	245 (82.77)	240 (97.96)	98 (40.83)	142 (59.17)
ipN1 x ipN1	380 (190, 190)	86	327 (86.05)	327 (100.00)	327 (100.00)	137 (41.90)	190 (58.10)
ipS1 x ipS1	344 (194, 150)	73	186 (54.07)	171 (91.93)	165 (96.49)	61 (36.97)	104 (63.03)
Reciprocal cross							
ilG1 x ipR1	382 (131, 251)	97	332 (86.91)	289 (87.05)	282 (97.57)	169 (59.93)	113 (40.07)
ipR1 x ilG1	393 (187, 206)	98	334 (84.99)	334 (100.00)	317 (94.91)	190 (59.94)	127 (40.06)
ilG1 x ipN1	402 (182, 220)	60	233 (57.96)	233 (100.00)	233 (100.00)	116 (49.79)	117 (50.21)
ipN1 x ilG1	263 (109, 154)	57	147 (55.89)	147 (100.00)	147 (100.00)	59 (40.14)	88 (59.86)
ilG1 x ipS1	309 (200, 109)	46	117 (37.86)	107 (91.45)	105 (98.13)	50 (47.62)	55 (52.38)
ipS1 x ilG1	308 (118, 190)	44	114 (37.01)	111 (97.37)	111 (100.00)	47 (42.34)	64 (57.66)

Table 3.3 (continued)

Crosses (Female x Male)	Total eggs (number)[a]	Embryonation rate[b]	Hatched n (%)	Pupation n (%)	Emergence n (%)	Total emergence n (%)	
						Female	Male
F_1- hybrid cross							
(ilG1 x ipR1)F_1 x (ilG1 x ipR1)F_1	352 (194, 158)	94	320 (90.91)	320(100.00)	314 (98.13)	157 (50.00)	157 (50.00)
(ipR1 x ilG1)F_1 x (ipR1x ilG1)F_1	341 (186, 155)	88	290 (85.04)	261 (90.00)	258 (98.85)	113 (43.80)	145 (56.20)
(ilG1 x ipN1)F_1 x (ilG1 x ipN1)F_1	324 (157, 167)	67	201 (62.04)	201 (100.00)	201 (100.00)	101 (50.25)	100 (49.75)
(ipN1 x ilG1)F_1 x (ipN1 x ilG1)F_1	347 (197, 150)	58	180 (51.87)	180 (100.00)	175 (97.22)	85 (48.57)	90 (51.43)
(ilG1 x ipS1)F_1 x (ilG1 x ipS1)F_1	347 (190, 157)	65	215 (61.96)	213 (99.07)	209 (98.12)	97 (46.41)	112 (53.59)
(ipS1 x ilG1)F_1 x (ipS1 x ilG1)F_1	348 (158, 190)	60	174 (50.00)	167 (95.98)	164 (98.20)	77 (46.95)	87 (53.05)

a: Two selective egg-batches of inseminated females from each cross; *b*: dissection from 100 eggs; n = number

3.8 DNA Sequence and Phylogenetic Analysis

The level of genetic distance and number of base substitutions between sequences of the 3 regions are presented in Tables 3.4-3.6. Analysis of the ITS2 sequence revealed no intraspecific sequence variation among the 3 and 5 isolines of *An. lesteri* and *An. paraliae*, respectively. Comparison of ITS2 sequences indicated that *An. lesteri* differed from *An. paraliae* by 16 base substitutions (pairwise distance = 0.040). In addition, 3 isolines of *An. lesteri* from Korea were identical with *An. lesteri* from China (= *Anopheles anthropophagus*) (AY803732, AY375467), Japan (AB159606) and Korea (EU789791), but they differed from those of the Philippines (AY375469) by 3 base substitutions (pairwise distance = 0.007). The average percentages of base composition for the ITS2 sequence of the 8 isolines (3 of *An. lesteri* from Korea and 5 of *An. paraliae* from Thailand) were: A, 29.9% (29.2–30.5%); T, 24.2% (23.6–24.9%); G, 25.2% (25.0-25.4%), and C, 20.8% (20.6-20.9%). Percentage of GC content was 46.0% in *An. lesteri* (448 bp) and 45.0% in *An. paraliae* (448 bp). All 8 sequences differed markedly from *An. sinensis* (pairwise distance = 0.321-0.338) and *An. peditaeniatus* (pairwise distance = 0.550-0.566) (Table 3.4). The analysis of COI (658 bp) among the 8 isolines revealed 4-9 base substitutions (pairwise distance = 0.007-0.017). On the contrary, *An. lesteri* and *An. paraliae* showed significant differences from *An. sinensis* (pairwise distance = 0.034-0.042) and *An. peditaeniatus* (pairwise distance = 0.037-0.041) (Table 3.5). The analysis of COII (685 bp) among the 8 isolines revealed 5-7 base substitutions (pairwise distance = 0.008-0.011). These 2 species also showed significant differences from *An. sinensis* (pairwise distance = 0.039) and *An. peditaeniatus* (pairwise distance = 0.031-0.036) (Table 3.6).

The NJ and Bayesian trees of *An. lesteri*, *An. paraliae*, *An. sinensis* and *An. peditaeniatus* were constructed based on the ITS2, COI and COII sequences (Figure 3.8). For ITS2, *An. lesteri* (n=8) and *An. paraliae* (n=5) were clustered in each monophyletic and well separated from *An. sinensis* and *An. peditaeniatus* with high bootstrap values (93-100%) in both NJ and Bayesian trees. The trees indicated that *An. lesteri* was more closely related to *An. paraliae* (average genetic distances = 0.038) than to the other species. Further, lower sequence divergences (0.000-0.002) were found within the population of each species. For COI and COII, the trees showed that *An.*

lesteri was more closely related to *An. paraliae* than to the other species with low level of average genetic distances (0.008-0.011) for both regions, while very low genetic distances (0.003-0.005) were obtained within the population of each species.

Table 3.4 Genetic distance and number of nucleotide substitutions in ITS2 sequences among *An. lesteri*, *An. paraliae*, *An. sinensis* and *An. peditaeniatus*

Taxon	1	2	3	4	5	6	7	8	9	10	11	12	13	14	15	16
1 ilG1		0	0	16	16	16	16	16	0	0	0	0	3	107	108	163
2 ilG2	0.000		0	16	16	16	16	16	0	0	0	0	3	107	108	163
3 ilG3	0.000	0.000		16	16	16	16	16	0	0	0	0	3	107	108	163
4 ipR1	0.040	0.040	0.040		0	0	0	0	16	16	16	16	17	110	111	160
5 ipR2	0.040	0.040	0.040	0.000		0	0	0	16	16	16	16	17	110	111	160
6 ipN1	0.040	0.040	0.040	0.000	0.000		0	0	16	16	16	16	17	110	111	160
7 ipS1	0.040	0.040	0.040	0.000	0.000	0.000		0	16	16	16	16	17	110	111	160
8 ipS2	0.040	0.040	0.040	0.000	0.000	0.000	0.000		16	16	16	16	17	110	111	160
9 anthC (AY803792)	0.000	0.000	0.000	0.040	0.040	0.040	0.040	0.040		0	0	0	3	107	108	163
10 anthC (AY375467)	0.000	0.000	0.000	0.040	0.040	0.040	0.040	0.040	0.000		0	0	3	107	108	163
11 lesJ (AB159606)	0.000	0.000	0.000	0.040	0.040	0.040	0.040	0.040	0.000	0.000		0	3	107	108	163
12 lesK (EU789791)	0.000	0.000	0.000	0.040	0.040	0.040	0.040	0.040	0.000	0.000	0.000		3	107	108	163
13 lesP (AY375469)	0.007	0.007	0.007	0.042	0.042	0.042	0.042	0.042	0.007	0.007	0.007	0.007		105	106	163
14 sinK (EU789790)	0.321	0.321	0.321	0.334	0.334	0.334	0.334	0.334	0.321	0.321	0.321	0.321	0.314		3	154
15 sinT (AY130473)	0.325	0.325	0.325	0.338	0.338	0.338	0.338	0.338	0.325	0.325	0.325	0.325	0.318	0.007		155
16 pedT (AB539061)	0.566	0.566	0.566	0.550	0.550	0.550	0.550	0.550	0.566	0.566	0.566	0.566	0.567	0.520	0.525	

Above triangle: number of nucleotide substitutions; below triangle: genetic distance

Table 3.5 Genetic distance and number of nucleotide substitutions in COI sequences among *An. lesteri*, *An. paraliae*, *An. sinensis* and *An. peditaeniatus*

Taxon	1	2	3	4	5	6	7	8	9	10
1 ilG1		1	2	7	6	6	8	7	22	22
2 ilG2	0.002		3	8	7	7	9	8	21	21
3 ilG3	0.004	0.006		5	4	4	6	5	20	22
4 ipR1	0.013	0.015	0.009		1	1	5	0	19	21
5 ipR2	0.011	0.013	0.007	0.002		0	4	1	18	20
6 ipN1	0.011	0.013	0.007	0.002	0.000		4	1	18	20
7 ipS1	0.015	0.017	0.011	0.009	0.007	0.007		5	22	20
8 ipS2	0.013	0.015	0.009	0.000	0.002	0.002	0.009		19	21
9 sinK (GQ265918)	0.042	0.040	0.038	0.036	0.034	0.034	0.042	0.036		29
10 PedT (AB539069)	0.041	0.039	0.041	0.039	0.037	0.037	0.037	0.039	0.055	

Above triangle: number of nucleotide substitutions; below triangle: genetic distance

Table 3.6 Genetic distance and number of nucleotide substitutions in COII sequences among *An. lesteri*, *An. paraliae*, *An. sinensis* and *An. peditaeniatus*

Taxon	1	2	3	4	5	6	7	8	9	10
1 ilG1		1	0	5	5	5	6	5	25	20
2 ilG2	0.002		1	6	6	6	7	6	25	20
3 ilG3	0.000	0.002		5	5	5	6	5	25	20
4 ipR1	0.008	0.009	0.008		0	0	5	0	25	22
5 ipR2	0.008	0.009	0.008	0.000		0	5	0	25	22
6 ipN1	0.008	0.009	0.008	0.000	0.000		5	0	25	22
7 ipS1	0.009	0.011	0.009	0.008	0.008	0.008		5	25	23
8 ipS2	0.008	0.009	0.008	0.000	0.000	0.000	0.008		25	22
9 sinK (AY130464)	0.039	0.039	0.039	0.039	0.039	0.039	0.039	0.039		29
10 PedT (AB539077)	0.031	0.031	0.031	0.034	0.034	0.034	0.036	0.034	0.045	

Above triangle: number of nucleotide substitutions; below triangle: genetic distance

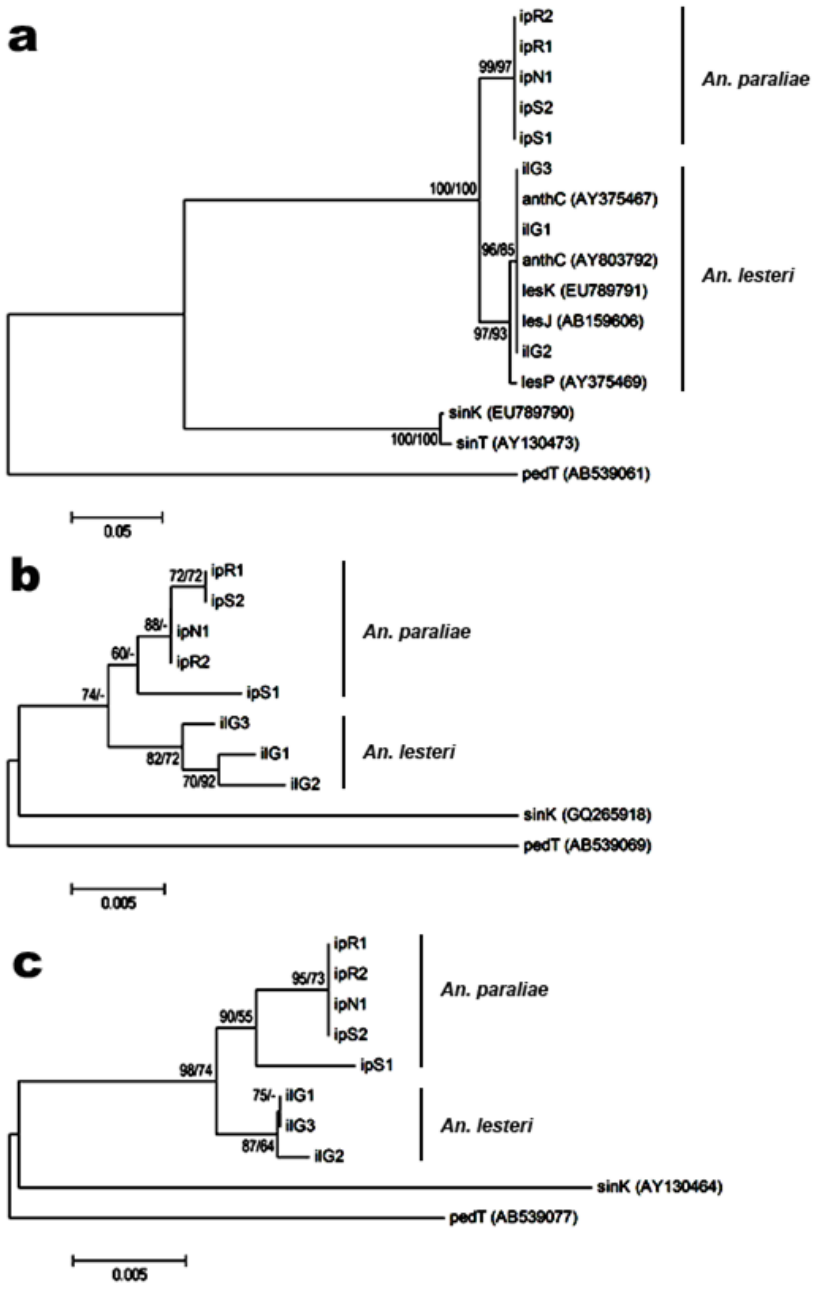

Figure 3.8 Neighbor-joining (NJ) trees inferred from sequences of three loci. A: second internal transcribed spacer; B: cytochrome *c* oxidase subunit I (COI); C: COII of *An. paraliae*, *An. lesteri*, *An. sinensis* and *An. peditaeniatus*. Numbers on branches are bootstrap values (%) of NJ analysis and Bayesian posterior probabilities (%). A hyphen (-) shows that the branch did not appear in majority rule (50%) consensus trees of Bayesian analysis. Branch lengths are proportional to genetic distance (scale bar)